"Ghost Introgression" As a Cause of Deep Mitochondrial Divergence in a Bird Species Complex

Dezhi Zhang,[1,2] Linfang Tang,[1,2] Yalin Cheng,[1,2] Yan Hao,[1,2] Ying Xiong,[1,2] Gang Song,[1] Yanhua Qu,[1] Frank E. Rheindt,[3] Per Alström,[1,4,5] Chenxi Jia,*[1] and Fumin Lei*[1,2,6]

[1]Key Laboratory of Zoological Systematics and Evolution, Institute of Zoology, Chinese Academy of Sciences, Beijing, China

[2]College of Life Sciences, University of Chinese Academy of Sciences, Beijing, China

[3]Department of Biological Sciences, National University of Singapore, Singapore

[4]Animal Ecology, Department of Ecology and Genetics, Evolutionary Biology Centre, Uppsala University, Uppsala, Sweden

[5]Swedish Species Information Centre, Swedish University of Agricultural Sciences, Uppsala, Sweden

[6]Center for Excellence in Animal Evolution and Genetics, Chinese Academy of Sciences, Kunming, China

*Corresponding authors: E-mails: jiacx@ioz.ac.cn; leifm@ioz.ac.cn.

Associate editor: Beth Shapiro

Abstract

In the absence of nuclear-genomic differentiation between two populations, deep mitochondrial divergence (DMD) is a form of mito-nuclear discordance. Such instances of DMD are rare and might variably be explained by unusual cases of female-linked selection, by male-biased dispersal, by "speciation reversal" or by mitochondrial capture through genetic introgression. Here, we analyze DMD in an Asian *Phylloscopus* leaf warbler (Aves: Phylloscopidae) complex. Bioacoustic, morphological, and genomic data demonstrate close similarity between the taxa *affinis* and *occisinensis*, even though DMD previously led to their classification as two distinct species. Using population genomic and comparative genomic methods on 45 whole genomes, including historical reconstructions of effective population size, genomic peaks of differentiation and genomic linkage, we infer that the form *affinis* is likely the product of a westward expansion in which it replaced a now-extinct congener that was the donor of its mtDNA and small portions of its nuclear genome. This study provides strong evidence of "ghost introgression" as the cause of DMD, and we suggest that "ghost introgression" may be a widely overlooked phenomenon in nature.

Key words: speciation, introgression, hybridization, mito-nuclear discordance, ghost mtDNA capture.

Introduction

Maternal inheritance and haploidy make lineage sorting of mitochondrial DNA (mtDNA) more rapid than that of nuclear DNA (nuDNA) (Avise 2000; Toews and Brelsford 2012), and have rendered mtDNA the workhorse of traditional phylogenetic research on recently diverged species (Zink and Barrowclough 2008). Yet, there have been reports of unusual cases in which deep mtDNA divergence can arise within a single panmictic species/population or between closely related species in the face of substantial nuclear gene flow (Spottiswoode et al. 2011; Hogner et al. 2012). This so-called deep mitochondrial divergence (DMD) can be considered a special case of mito-nuclear discordance (Toews and Brelsford 2012) and involves cases in which the actual divergence between populations or taxa is believed to be substantially shallower than indicated by mtDNA. Reported examples of DMD abound in birds (Rheindt and Edwards 2011; Spottiswoode et al. 2011; Webb et al. 2011; Hogner et al. 2012; Dai et al. 2013; Pavlova et al. 2013; Fossøy et al. 2016), and the phenomenon has also been found in other groups of organisms, such as invertebrates (Kvie et al. 2012; Giska et al. 2015) and plants (Huang et al. 2014) (albeit in their plastomes, not mtDNA genomes).

The Tickell's leaf warbler *Phylloscopus affinis* species complex is an assemblage of East Asian leaf warblers (Aves, Phylloscopidae) (Martens et al. 2008), comprising three species by current taxonomic standards: *P. affinis*, *P. occisinensis*, and *P. griseolus* (Clements et al. 2018; Gill and Donsker 2019) (hereafter the shortened taxon names *affinis*, *occisinensis*, and *griseolus* are used). Their breeding ranges are approximately circularly distributed around the Qinghai-Tibet Plateau (fig. 1a). Because of phenotypic similarities with Himalayan *affinis*, the more easterly *occisinensis* remained unrecognized until 2008, when Martens et al. (2008) described it as a new species, mainly on the basis of substantial mitochondrial divergence. However, its recognition as a distinct species remains contested (del Hoyo and Collar 2016). Applying a mutation rate of 2.1% per million years to mitochondrial *cytochrome-b* (CYTB) sequences suggests that the divergence time between *occisinensis* and *affinis* was over 4 My (Alström et al. 2018). In contrast, the divergence estimate for this split based on nuclear sequences is much shallower (supplementary fig. S1, Supplementary Material online), indicating potentially unresolved DMD in these birds. Moreover, phylogenetic relationships among *occisinensis*, *affinis*, and *griseolus* have emerged inconsistent when comparing the signal of
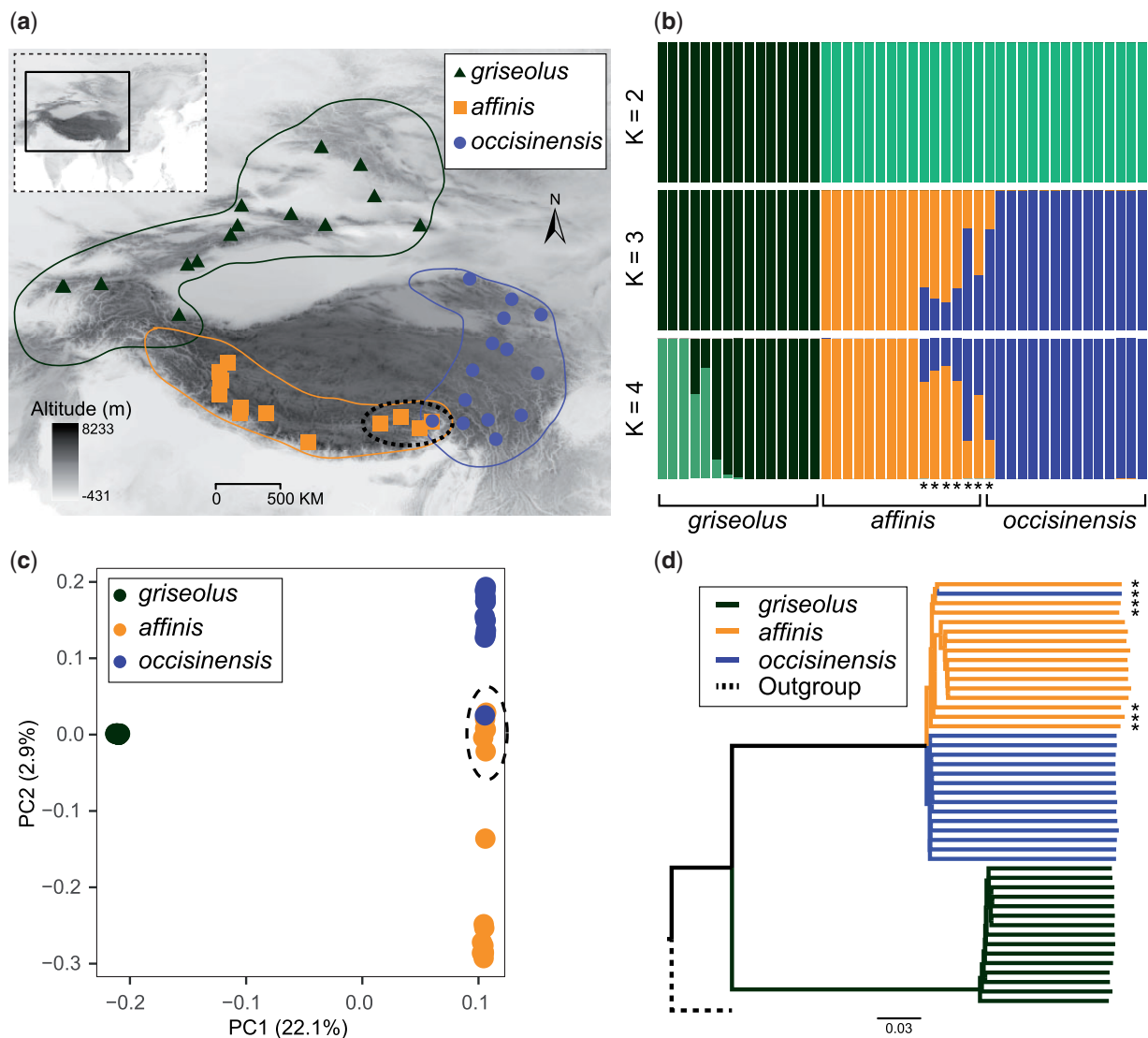
FIG. 1. DNA sampling localities and population structure of the *Phylloscopus affinis* species complex. (*a*) DNA sampling localities and the approximate breeding ranges for the three taxa; the black box in the top left map represents the study area. (*b*) Genetic structure based on genome-wide SNPs estimated in FRAPPE 1.1 at *K* = 2, 3, and 4, respectively. (*c*) Principal Component Analysis based on genome-wide SNPs performed in GCTA 1.24. (*d*) Neighbor-joining tree estimated in TreeBeST 1.9.2 based on concatenated SNPs for all 45 samples. The dashed lines in (*a*) and (*c*) and the asterisks in (*b*) and (*d*) denote presumably admixed individuals from the Lhasa–Nyingchi area. Taxon names are defined by mitochondrial haplotypes.

mitochondrial genes (Martens et al. 2008) with that of combined mtDNA and nuclear markers (Päckert et al. 2012; Alström et al. 2018) or even among different analyses of the same multilocus data set (Alström et al. 2018).

Given the sparse and stochastic sampling of nuclear markers in previous studies (Päckert et al. 2012; Alström et al. 2018), *affinis* and *occisinensis* may represent two deeply diverged sister species. However, if mito-nuclear discordance persists in the face of genome-wide data, several alternative hypotheses may apply. First, DMD may arise if the divergence of mtDNA predated nuclear differentiation. For instance, studies of brood-parasitic birds have revealed that DMD could reflect the ancient divergence and maintenance of females' choice of host species (Spottiswoode et al. 2011; Fossøy et al. 2016). Second, male-biased dispersal may maintain cohesion in nuDNA in the absence of mtDNA gene flow

(Dai et al. 2013) if males of both *affinis* and *occisinensis* range widely and mate freely while females remain restricted in their movements. Third, DMD may reflect "speciation reversal" (Webb et al. 2011), that is, the two taxa may have diverged long ago, but later merged. If mtDNA is neutral or under weak selection, strong phylogeographic structure can arise (Irwin 2002, 2012), followed by intense episodes of continuous gene flow homogenizing nuclear but not mitochondrial genomes (Hogner et al. 2012; Toews et al. 2016). Lastly, one of the two deeply diverged mitochondrial lineages may have been captured through genetic introgression from an extinct congeneric species (Hogner et al. 2012). Given that all closely related extant *Phylloscopus* species are believed to have been sampled mitochondrially (Olsson et al. 2005; Johansson et al. 2007; Martens et al. 2008; Päckert et al. 2012; Alström et al. 2018),

one of the two deeply diverged mitochondrial lineages could have originated from an extinct species. This would represent a special case of "speciation reversal," in which the resultant lineage mostly carries the DNA of one of the two parent species, while the other parent species is merely reflected in a minute proportion of the entire genome, such as mainly the mitochondrial genome. For example, one of two deeply diverged plastomes between two closely related *Populus* species is thought to be derived from plastid capture from an extinct poplar (Huang et al. 2014). Similarly, the strong divergence between older and more recent Neanderthal mito-lineages is attributed to mitochondrial introgression from modern humans into recent Neanderthals (Hajdinjak et al. 2018). If DMD between *affinis* and *occisinensis* is attributable to mitochondrial capture from an extinct species, we expect certain levels of accompanying nuclear introgression from the extinct species that may manifest itself in outlier peaks of sequence divergence (D_{XY} and the relative node depth) and an increase of relative differentiation (F_{ST}) between *affinis* and *occisinensis* in introgressed genomic regions.

Using morphological, bioacoustic and resequenced genomic data, we unravel a case of DMD between the leaf warbler taxa *affinis* and *occisinensis* and shed light on its most likely cause. Examining various hypotheses, we lay out the case for DMD caused by mtDNA capture from an extinct *Phylloscopus* species under the scenario of a moving hybrid zone, in which the population denoted by *affinis* originated from the westward dispersal of the eastern ancestral population (present-day *occisinensis*) into the range of a now extinct species, and in which the extinct species left its mtDNA and small portions of the nuclear genome in *affinis*.

Results

MtDNA Divergence

We resequenced genomes of 15 males for each of the three taxa, covering most of the breeding range of the *P. affinis* species complex (fig. 1*a*). A total of 885.9 Gb and an individual average of 19.7 Gb of paired-end reads were obtained (supplementary table S1, Supplementary Material online). We assembled mitochondrial genomes from the resequenced data for each individual using MITObim 1.8 (Hahn et al. 2013), and used the 13 protein-coding gene sequences (NCBI GenBank accession numbers: MK360182–MK360766) to infer phylogenetic tree. Three strongly supported monophyletic groups were recovered based on the matrix of 13 mitochondrial protein-coding genes (fig. 2*a*). The *affinis* and *occisinensis* clades were sisters, and the *griseolus* clade was sister to these two (fig. 2*a*). The mitochondrial divergence time between *affinis* and *occisinensis* was estimated at ~3.1 My (95% highest posterior density [HPD]: 2.6–3.6 My), and ~3.3 My (95% HPD: 2.7–3.8 My) between *griseolus* and the former two taxa (fig. 2*a*). The uncorrected mitochondrial pairwise distance was 0.078 between *affinis* and *occisinensis*, 0.082 between *griseolus* and *affinis*, and 0.083 between *griseolus* and *occisinensis*.

NuDNA Structure

Mapping resequenced data to the reference genome of *P. sibilatrix* (Bird 10,000 Genomes Project, unpublished, scaffold N50 = ~330 kb) resulted in an average depth and breadth of coverage at 10.9% and 94.9%, respectively, with an average mapping rate of 82.0% (supplementary table S1, Supplementary Material online). We identified a total of 13,257,493 high-quality SNPs after filtering.

Population structure analysis using FRAPPE (Tang et al. 2005) showed that *affinis* and *occisinensis* form one group at $K = 2$, while *griseolus* clusters apart (fig. 1*b*). At $K = 3$ and $K = 4$, FRAPPE revealed that all seven individuals around the contact zone between *affinis* and *occisinensis* (Lhasa–Nyingchi area, dashed line in fig. 1*a*; labeled with asterisks in fig. 1*b*) exhibited admixture between *affinis* and *occisinensis*; one of these individuals carried *occisinensis* mtDNA whereas the remaining six had *affinis* mtDNA. Similarly, in PCA, *griseolus* formed a separate cluster along principal component (PC) 1, whereas *affinis* and *occisinensis* could only be discriminated along PC2, where the seven admixed individuals (dashed line) uncovered by FRAPPE also occupied an intermediate position (fig. 1*c*). The neighbor-joining tree based on concatenated genome-wide SNPs recovered a single clade with minimal differentiation between *affinis* and *occisinensis*, with *griseolus* in a deeply diverged sister clade, and with all the individuals identified as admixed by FRAPPE (fig. 1*d*) forming part of *affinis*. Species tree analysis (excluding the seven individuals from the Lhasa–Nyingchi area) indicated that *affinis* and *occisinensis* were sister taxa, with a divergence time of only 6,000 years (95% HPD: 0.004–0.008 My), whereas *griseolus* was sister to these, with a divergence time of 2.1 My (95% HPD: 1.9–2.3 My) (fig. 2*b*). The mean F_{ST} between *griseolus* and nonadmixed *affinis* was 0.38, between *griseolus* and nonadmixed *occisinensis* 0.37, but between nonadmixed *affinis* and *occisinensis*, it was an order of magnitude lower at only 0.03. The mean F_{ST} between the group of individuals identified as admixed in FRAPPE (indicated by asterisks; fig. 1*b*) and the two nonadmixed groups was 0.016 and 0.012, respectively.

Gene Flow Test within the *P. affinis* Species Complex

Population structure analysis revealed the existence of three groups within the *P. affinis* species complex: *griseolus*, *affinis*, and *occisinensis*. The latter two groups are bridged by a mixed population from the Lhasa–Nyingchi area (the intermediate group). We tested multiple divergence models (supplementary fig. S2, Supplementary Material online) between *affinis* and *occisinensis*, excluding the intermediate individuals, using ∂a∂i (Gutenkunst et al. 2009). The strict isolation model with no migration (SI) displayed the poorest fit, whereas all models incorporating gene flow and population size change generally exhibited a much better fit to the data (supplementary table S2, Supplementary Material online). Among the gene flow models, the SCa_pop model (secondary contact with asymmetric migration and population size change; supplementary fig. S2, Supplementary Material online) narrowly emerged ahead of the other models (supplementary fig. S3 and table S2, Supplementary
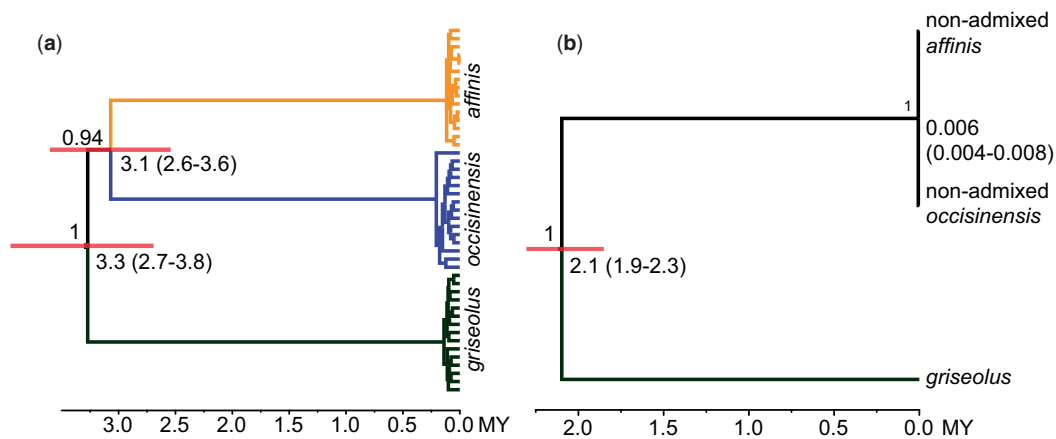
FIG. 2. Phylogeny and divergence time. (*a*) Bayesian tree (BEAST) based on 13 mitochondrial protein-coding genes. (*b*) species tree (*BEAST) based on 188 nuclear introns. Posterior probabilities are shown above the main nodes, and divergence times with 95% highest posterior density (HPD) are shown below these nodes (95% HPD also indicated by horizontal bars). Time scale in millions of years.

Material online). This best-fit model suggested that both taxa's population sizes increased from the split to the present. Using the parameters estimated from the SCa_pop model (supplementary table S3, Supplementary Material online), we calculated the divergence time between *affinis* and *occisinensis*, specifically applying a generation time (g) of 1.7 years (Bensch et al. 1999), a mutation rate (μ) of 0.33% per million years (Zhang et al. 2014), and a sequence length (L) for the SNP data set output of 1×10^9 (approximately equivalent to genome size). Using the equation (Gutenkunst et al. 2009) divergence time = $2 N_{ref} \times (T1+T2) \times g$, we obtained a divergence time estimate of ~85,445 years between *affinis* and *occisinensis* (N_{ref}, T1, and T2 represent the reference effective population size, the scaled time between the split and the secondary contact and the scaled time between the secondary contact and present, respectively; supplementary table S3, Supplementary Material online).

To test whether historical gene flow occurred between *griseolus* and *affinis*/*occisinensis* during their divergence, we applied an ABBA-BABA test (also known as *D*-statistic; Green et al. 2010; Durand et al. 2011) in ANGSD 0.902 (Korneliussen et al. 2014). When we set nonadmixed *occisinensis* as P1, nonadmixed *affinis* as P2, and *griseolus* as P3, *D*-statistic and *Z*-score values of all combinations were >0 and >3, respectively, indicating significant historical gene flow between *affinis* and *griseolus*. The average *D*-statistic and *Z*-score values were 0.0267 and 24.75, respectively (supplementary table S4, Supplementary Material online).

Linkage Disequilibrium and PSMC Analyses

Our main hypothesis is that *affinis* originated from a westward dispersing subpopulation of an ancestral population (hereafter referred to as "proto-Tickell's" warbler) expanding into the range of a now-extinct species which interbred with and left its mtDNA in *affinis* (fig. 3). This hypothesis leads to a prediction that *affinis* would display higher linkage disequilibrium (LD) and a lower effective population size (N_e) than *occisinensis*.

LD, measured as the correlation coefficient (r^2) for <500 base pair (bp) across the genome, is <0.2 for all four groups (nonadmixed *affinis*, nonadmixed *occisinensis*, admixed individuals, and *griseolus*), with *occisinensis* showing the lowest overall LD (fig. 4). We conducted PSMC analysis (Li and Durbin 2011) to infer demographic histories of our target taxa, showing that all three taxa have experienced a slow and steady population expansion (fig. 5). The taxon *griseolus* was inferred to have maintained a relatively stable effective population size into the present. In contrast, both *affinis* and *occisinensis* experienced a rapid decline in effective population size around the build-up to the peak of the last ice age (~30–50 Ka). Then the latter two groups underwent a re-expansion, which was more intense in *occisinensis*. The taxon *affinis* showed an additional decline in effective population size ~20 Ka that has lasted until the present day (fig. 5).

Distribution of Outliers of D_{XY} and Relative Node Depth between *affinis* and *occisinensis*

Despite the presence of multiple highly differentiated genomic regions, the background level of genomic differentiation between nonadmixed *affinis* and *occisinensis* was generally extremely low (fig. 6). We plotted the outliers of absolute differentiation D_{XY} against the corresponding relative differentiation F_{ST} for 100-, 50-, 10-, and 2-kb windows, respectively, across the genome. For 2-kb genomic window sizes, we found that D_{XY} outliers were generally constant in magnitude with increasing F_{ST} (fig. 7), a phenomenon that is consistent with outliers of genomic differentiation resulting from a one-time introgression event. As D_{XY} may be strongly influenced by mutation rate variation along the genome, we also calculated outliers of relative node depth (RND), a measure of sequence divergence corrected for mutation rate variation (Feder et al. 2005). The pattern for RND resembled that of D_{XY} (supplementary fig. S4, Supplementary Material online).

We then tested whether *griseolus* could have been the donor lineage of these D_{XY} outliers. Under the latter scenario, the background level of genomic differentiation between nonadmixed *affinis* and *griseolus* would exceed D_{XY} in the genomic outliers flagged earlier between nonadmixed *affinis* and *occisinensis*. However, differentiation at the flagged
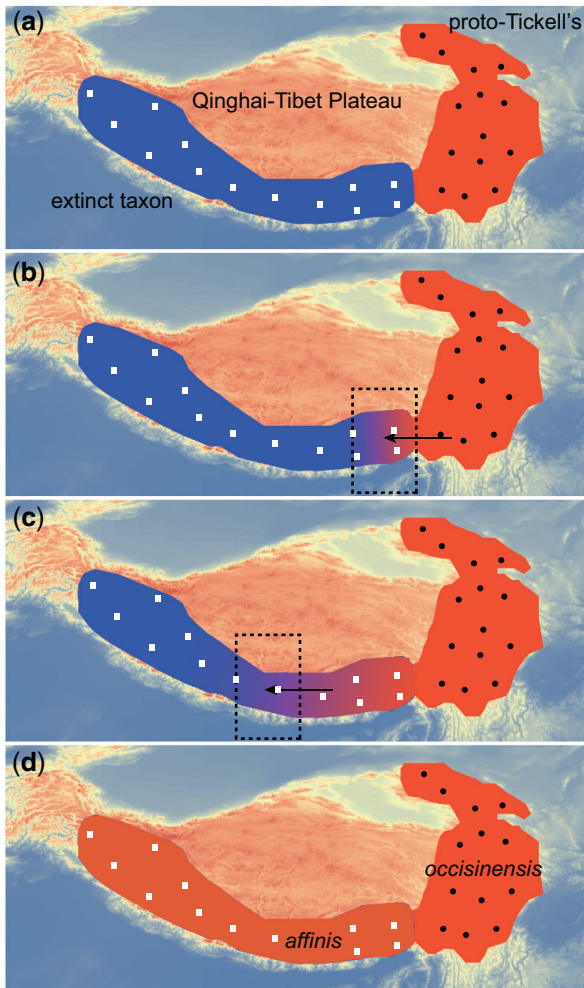
Fig. 3. Schematic diagram of the proposed moving hybrid zone scenario. (*a*) The ancestral population of *affinis* and *occisinensis* ("proto-Tickell's") lived in the east of the range, and the extinct taxon lived in the west of the range, with distinct mtDNA haplotypes indicated by black circles and white squares, respectively. (*b*) "proto-Tickell's" started expanding westwards into the distribution of the now extinct taxon in the wake of a hybrid zone (dotted box area). (*c*) The hybrid zone continued moving westwards. (*d*) The extinct taxon is entirely replaced but has left its mtDNA in *affinis* as a "ghost of introgression past."
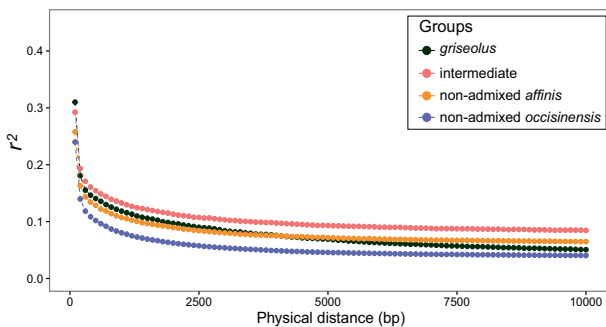

Fig. 4. Linkage disequilibrium decay for four groups within the *Phylloscopus affinis* species complex. The horizontal and vertical axes indicate physical distance (bp) and r^2 values (the correlation coefficient), respectively.
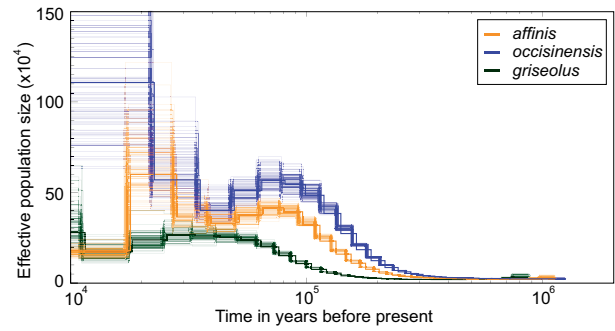

Fig. 5. PSMC estimates of change in effective population size for the three taxa within the *Phylloscopus affinis* species complex. Thick and thin lines of the same color represent the median and 100 rounds of bootstrapping results, respectively.

outliers in fact exceeded background differentiation in pairwise analyses between nonadmixed *affinis* and *griseolus*, refuting the hypothesis that *griseolus* introgression could have caused these specific D_{XY} outliers (supplementary fig. S5, Supplementary Material online, Wilcoxon rank sum test, $P < 2.2 \times 10^{-16}$).

Hybrids of Early Generation Test
The R package HIest (Fitzpatrick 2012) was used to test whether the seven intermediate individuals between *affinis* and *occisinensis* were early generation hybrids. We identified that none of the seven individuals was classified as an F_1, F_2, or first or second generation backcross (supplementary table S5, Supplementary Material online), suggesting that gene flow between *affinis* and *occisinensis* may be limited or not currently ongoing in the sampling area around Lhasa–Nyingchi.

Phenotypic Divergence
We conducted linear discriminant analysis (LDA) for morphometric traits (supplementary table S6, Supplementary Material online), plumage colors (supplementary table S7, Supplementary Material online), and songs (supplementary table S8, Supplementary Material online) to estimate phenotypic divergence within the *P. affinis* species complex. The LDA of morphometric traits indicated that *griseolus* can be distinguished from *affinis* and *occisinensis*, while the latter two taxa are indistinguishable from each other on measurements (fig. 8*a*). All nine individuals from the Lhasa–Nyingchi area identified as putatively admixed were indistinguishable from the two parental groups (fig. 8*a*). Plumage color resembled morphometry in pattern: *griseolus* was clearly distinguishable from *affinis* and *occisinensis*, whereas the latter two were not clearly separable (fig. 8*b*). As with morphometry, all 13 putatively admixed individuals from the Lhasa–Nyingchi area were indistinguishable from the two parental groups (fig. 8*b*). The taxon *griseolus* was also clearly separable from *affinis* and *occisinensis* based on song, while the latter two groups were only clinally differentiated from each other in bioacoustics, with distinct overlap in parameters, especially among the putatively admixed individuals from the Lhasa–Nyingchi area (fig. 8*c*).
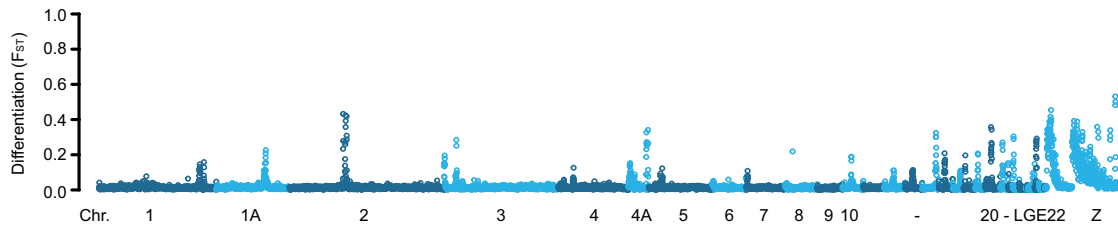
FIG. 6. Genomic differentiation between nonadmixed *affinis* and *occisinensis* along the genome based on 100-kb sliding windows. The vertical axis indicates F_{ST}. Alternating colors indicate different chromosomes with labels underneath.
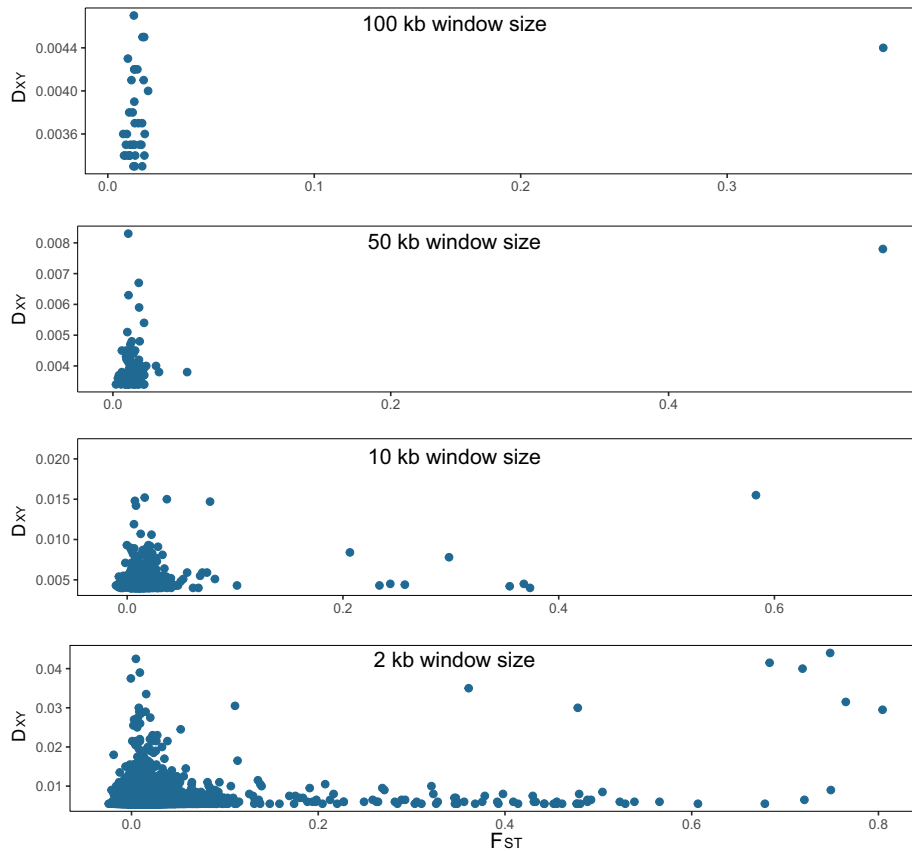

FIG. 7. Outliers of D_{XY} between nonadmixed *affinis* and *occisinensis* plotted against their corresponding F_{ST}, with decreasing genomic window size from top to bottom.

Discussion

Since the early days of DNA sequencing, estimation of mtDNA divergences has served as a biological yardstick for species determination in the animal kingdom, including birds. This practice was particularly common at a time when mtDNA was the major data type available for traditional phylogenetic studies (Zink and Barrowclough 2008), although the occasional occurrence of DMD has led to obvious cases of discordance between mtDNA and nuDNA (Spottiswoode et al. 2011; Webb et al. 2011; Fossøy et al. 2016). Here, we demonstrate that the *P. affinis* leaf warbler complex is such an example of DMD. Throughout the 20th century, the *P. affinis* complex was thought to be composed of two species, *affinis* and *griseolus*, based on differences in morphology, song, habitat choice, and behavior. *Phylloscopus occisinensis* was only

recently recognized as an independent species, mainly on the basis of its substantial mtDNA divergence from the other two species (Martens et al. 2008). In this study, we confirm this instance of DMD between *affinis* and *occisinensis* on the basis of genomic and phenotypic inquiry. The analysis of 13 mtDNA protein-coding genes suggests a roughly equally deep divergence among all three lineages (*affinis*, *occisinensis*, and *griseolus*) (fig. 2a). However, the two former taxa are virtually identical in body measurements and plumage, and exhibit clinal song differences across their vast geographic distribution range, with bioacoustic intermediacy in areas of contact, while showing pronounced distinctions from the third lineage *griseolus* in these traits (fig. 8). Akin to the phenotypic analyses, the analyses of genomic data also suggest limited differentiation between *affinis* and *occisinensis*,
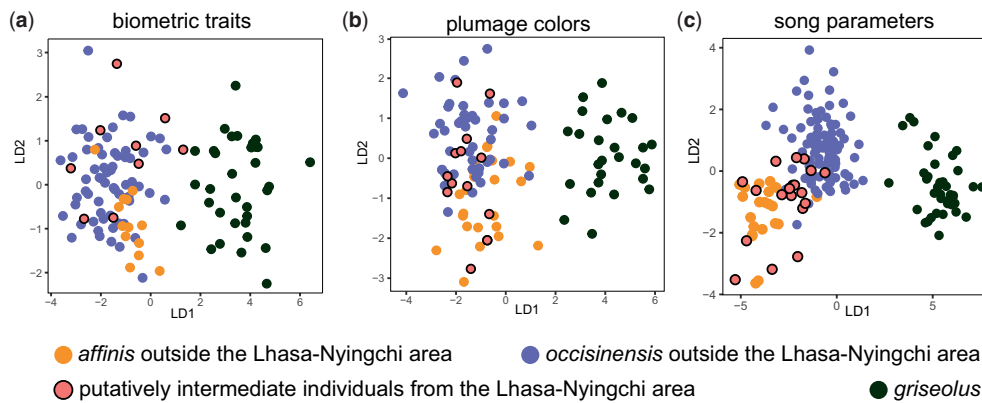
Fig. 8. Linear discriminant analysis of phenotypic traits within the *Phylloscopus affinis* species complex. (*a*) Biometric traits. (*b*) Plumage colors. (*c*) Song parameters.

whereas *griseolus* is deeply diverged (figs. 1*c* and *d* and 2*b*). In summary, DMD has misled taxonomists into classifying *occisinensis* as a distinct species. Given that nuclear and phenotypic differentiation are insignificant in comparison to mtDNA divergence, this is a classical case of mito-nuclear discordance.

Several hypotheses may account for DMD between *affinis* and *occisinensis*. 1) Ancient mtDNA divergence hypothesis: studies of brood-parasitic birds have demonstrated ancient divergence of strictly female-linked traits, such as mtDNA and the W chromosome, as a result of differential host choice (Spottiswoode et al. 2011; Fossøy et al. 2016). Inspection of the W chromosome was not possible in our study as all individuals were male. However, this scenario is highly improbable in our case, as this is an exceptional phenomenon that is strictly associated with unusual life-history traits such as brood parasitism that have never been demonstrated in conventional birds such as *Phylloscopus* leaf warblers. Moreover, under this hypothesis, males would freely mate with females with different female-linked traits, leading to a sympatric distribution of the two deeply diverged mtDNA lineages. 2) Male-biased dispersal hypothesis: rampant male dispersal in the face of strict female philopatry may also cause DMD. However, such extreme differences in sex-specific dispersal as would be required to generate this pattern are highly exceptional in birds, especially in songbirds that are generally characterized by female-biased dispersal (Clarke et al. 1997). 3) "Speciation reversal" hypothesis: at the early stages of "speciation reversal," the continuous nuclear gene flow without mitochondrial gene flow may also generate DMD between *affinis* and *occisinensis*. This is not likely because it is hard to maintain the slight divergence between them in the face of several million years hybridization, on the contrary, they would rather merge or separate. 4) A special case of "speciation reversal"—"ghost introgression" hypothesis: mtDNA capture through genetic introgression is a widespread phenomenon in animals (Toews and Brelsford 2012) that has—by now—been implicated in numerous bird lineages (Rheindt and Edwards 2011). Its detection is challenging but feasible when the mtDNA donor is an extant species (Rohwer et al. 2001); however, when the donor species is

extinct, firm proof for mtDNA capture is hard in the absence of fossil DNA material. However, there are multiple lines of evidence that suggest that *affinis* is the product of a moving hybrid zone expansion of the ancestral population of *affinis* and *occisinensis* ("proto-Tickell's warbler") into the more western range of an extinct species that formerly occupied *affinis*'s range but that was eventually replaced by the invading "proto-Tickell's" population (Currat et al. 2008; Rheindt and Edwards 2011) (fig. 3). In the process, the mtDNA from the receding, now extinct, species introgressed into the invading species (Krosby and Rohwer 2009; Seixas et al. 2018), resulting in the present-day DMD between *affinis* and *occisinensis*.

The taxon *affinis* exhibits elevated genome-wide levels of LD and lower N_e as compared with *occisinensis* (figs. 4 and 5). This pattern conforms to a scenario in which an ancestor which lived in the east of the range started expanding westwards into the distribution of a now extinct species and replaced it (fig. 3). The taxon *occisinensis* would thereby constitute a genetically diverse population with an overall low genomic LD that continues to live in the ancestral range, whereas *affinis* is a genetically more impoverished population with a higher genome-wide LD that has only recently become established in its current home range. This scenario is akin to the classic situation in African and non-African humans (Reich et al. 2001). As has been shown in hominids (Currat et al. 2008; Currat and Excoffier 2011), the extinct species would have left behind small parts of its genetic material (e.g., mtDNA) in the resulting taxon *affinis* as a "ghost of introgression past" (Rheindt and Edwards 2011).

The nuclear genome presumably holds the key to demonstrating the likelihood of "ghost introgression" from an extinct species as an explanation for DMD. We found that outliers of D_{XY} and RND between *affinis* and *occisinensis* were generally constant in magnitude along with increasing F_{ST} at 2-kb window size (fig. 7). This pattern conforms to a scenario in which "ghost introgression" introduced these highly divergent genomic fragments at one point of time that is reflected in the largely similar magnitude of D_{XY} and RND outliers, while F_{ST} is not expected to be equal among these differentiation peaks because it additionally reflects genetic diversity within each

population. More importantly, if these D_{XY} and RND peaks were independent of an introgression event and constituted the product of random positive selection pressures on various parts of the genome, D_{XY} and RND peaks would not be expected to cluster with increasing F_{ST} as much as they do. We further tested whether the introgression event that introduced these deeply diverged genomic windows could have been contributed by *griseolus*, given that we have independently detected historical nuclear-genomic introgression between *griseolus* and *affinis* on the basis of an ABBA-BABA test (supplementary table S4, Supplementary Material online). Under this scenario, divergence between *griseolus* and *affinis* across the previously flagged D_{XY} outliers should be much shallower than genomic background divergence. Instead, D_{XY} across these windows emerged as significantly higher than background differentiation (supplementary fig. S5, Supplementary Material online), ruling out *griseolus* as a potential introgression donor specifically of these windows of elevated differentiation. Our detection of constant-sized outliers of D_{XY} and RND at smaller (2 kb) rather than larger window sizes indicates a more ancient introgression event between *affinis* and the "ghost species" that would allow for recombination to break apart initially longer introgressed fragments into ever smaller sections over time. The demonstration of historical introgression between *griseolus* and *affinis* is further corroboration that genetic introgression is present in this particular clade of *Phylloscopus* warblers.

Introgression between closely related species during the early stages of speciation is widely appreciated (Payseur and Rieseberg 2016), and it can be detected between distantly related species (Zhang et al. 2016) or between deep ancestral lineages (MacGuigan and Near 2019). Although extinction is pervasive in nature, the incidence of "ghost introgression" may remain seriously underestimated based on the unavailability of ancient DNA of extinct species. Introgression from extinct hominids into modern humans is now a well-established fact largely thanks to human population-genomicists' ability to leverage the information content of fossil DNA (Green et al. 2010; Huerta-Sánchez et al. 2014). Fortunately, recently developed analytical approaches make it feasible to detect introgression from extinct species without fossil DNA in hominids (Kuhlwilm et al. 2019), which possess a wealth of genomic data and high-quality genome assembly as compared with nonmodel systems. With the rising availability of genomic data on nonmodel organisms, our study suggests that "ghost introgression" will be increasingly recognized as an important phenomenon shaping the modern tree of life.

Materials and Methods

Sampling and Whole-Genome Resequencing

We sampled a total of 45 male individuals from three taxa, *affinis*, *occisinensis*, and *griseolus* (15 individuals from each taxon) (fig. 1*a*; supplementary table S1, Supplementary Material online). Total genomic DNA was extracted from muscle tissue using the Tissue/Cell Genomic DNA Extraction Kit (Aidlab Biotechnologies Co. Ltd., Beijing, China) according to the manufacturer's protocol. Total

DNA was randomly sheared by ultrasonication. DNA libraries with ~350 bp insertions were constructed. All libraries were sequenced using Illumina HiSeq-X10 with a paired-end read length of 150 bp on seven lanes in Berry Genomics (Beijing, China). Raw reads were processed to remove adapter sequences, low-quality reads (those with over 50% of bases having Phred quality scores <3) and poly-N reads (those with ≥3% unidentified nucleotides) using in-house scripts. The raw sequence data produced in this study were deposited at the NCBI Sequence Read Archive (SRA) under SRA accession: SRP140017.

SNP Calling

Quality controlled reads were mapped to the reference assembly of a congeneric species (*P. sibilatrix*) using BWA 0.7.12 (Li and Durbin 2009). The divergence time between *P. sibilatrix* and the *P. affinis* species complex has been estimated at ~8.5–12.5 My based on a mitochondrial CYTB clock rate of 2.1% per million years (Alström et al. 2018). *Phylloscopus trochiloides* (NCBI Sequence Read Archive: SRR1172475) (Alcaide et al. 2014) was used as an outgroup. Variants were called in SAMtools 0.1.19 (Li et al. 2009) using the "mpileup" module for all 46 samples with the settings "mpileup -g -u -S –D." PCR duplicates were removed before variant calling in SAMtools 0.1.19 (Li et al. 2009) with the "rmdup" command. SNPs were filtered using VCFtools 0.1.12b (Danecek et al. 2011) and bcftools (Li et al. 2009) according to the following criteria: 1) only biallelic SNPs were retained; 2) quality value ≥30; 3) genotype depth ≥5; 4) no missing genotype was allowed (leading to the discarding of a SNP site when only a single individual was missing); 5) SNPs differing in the reference species but otherwise homogeneous were filtered out; and 6) SNPs differing in the outgroup but homogeneous within the *P. affinis* complex were also filtered out.

Population Structure and Divergence Analyses

The concatenated nuclear SNPs were used to infer a neighbor-joining (NJ) tree using TreeBeST 1.9.2 (Vilella et al. 2008) with *P. trochiloides* as an outgroup. FRAPPE 1.1 (Tang et al. 2005) was used to analyze population structure within the *P. affinis* species complex with *K* values ranging from 2 to 4 and a maximum of 10,000 iterations. Principal Component Analysis (PCA) was performed using GCTA 1.24 (Yang et al. 2011). The fixation index F_{ST} (Weir and Cockerham 1984) was estimated in VCFtools 0.1.12b (Danecek et al. 2011) to infer population differentiation. SNPs with a minor allele frequency ≤ 0.05 were removed, as rare variants may influence F_{ST} estimation (Bhatia et al. 2013). Mean F_{ST} was estimated for each pairwise combination of the four groups identified in the PCA (see Results).

We used introns, which are generally thought to be neutrally evolved, to estimate the divergence time between each taxon pair in the *P. affinis* species complex. SOAPdenovo 2.04 (Luo et al. 2012) was utilized to assemble scaffold-level genome sequences for each individual using default parameters with a k-mer value of 25. We used GenBlast 1.0.138 (She et al. 2008) to infer the positions of homologous genes based on

the longest coding (CD) sequences of each gene of the great tit *Parus major* (Laine et al. 2016), as *Parus major* is phylogenetically closest to the focal species complex among the most well assembled and annotated bird genomes currently available. We then applied exonerate 2.2.0 (Slater and Birney 2005) to predict the positions of introns for each gene based on the same CD sequences of *Parus major*. After extracting the intron sequences of each individual, we selected one random individual and performed mutual BLAST with the remaining individuals using BLAST+ 2.2.26. To increase computational efficiency and to obtain higher numbers of homologous introns, only five individuals from each *griseolus*, *affinis*, and *occisinensis* were used. The seven samples from the Lhasa–Nyingci area with evidence of admixture (see Results) were excluded from this analysis. In the end, we obtained 188 introns with an average length of 947 bp (in total ∼178 kb). *BEAST (Heled and Drummond 2010) as implemented in BEAST 2.4.5 (Bouckaert et al. 2014) was used in combination with a GTR substitution model to infer the species tree and estimate divergence times based on all the partitioned introns. The clock model was set to a strict clock with a passerine clock rate of 0.33% per million years (Zhang et al. 2014), and a Yule speciation model and population size model of linear and constant root were employed. We carried out ten million runs, sampling every 5,000 generations with a burn-in of 10%. The consensus tree was generated in TreeAnnotator 1.8.

MtDNA Divergence Estimation

The mitochondrial genome for each individual was assembled using MITObim 1.8 (Hahn et al. 2013), which relies on the sequence assembler MIRA 4.0.1 (Chevreux et al. 1999). The complete mitochondrial genome of a congeneric species, *P. inornatus* (GenBank: KF742677.1), served as the reference. As MIRA is sensitive to the minority proportion of reads and the initially assembled mitochondrial genome sequences contained many ambiguous sites, we used the command "miraconvert" to convert these ambiguities into homozygous sites. Mitochondrial sequences were aligned using ClustalW as implemented in MEGA 6.06 (Tamura et al. 2013) and manually trimmed. For each individual, we then manually annotated protein-coding genes using alignments with *P. inornatus* mitochondrial protein sequences for use in downstream analysis.

BEAST 2.4.5 (Bouckaert et al. 2014) was used to infer phylogenetic trees using the 13 partitioned mtDNA protein-coding genes. Ten million iterations were carried out while sampling every 1,000 generations. We utilized a GTR model for all genes and applied the widely used clock rate of 2.1% per million years for CYTB (Weir and Schluter 2008), while leaving the evolutionary rate of other genes to be estimated. Convergence of posterior distributions was assured by requiring the effective sample size to be >200 and by monitoring trace plots (reaching stability) in Tracer 1.6. A consensus tree was generated using TreeAnnotator 1.8 with a 20% burn-in, and was visualized in FigTree 1.3.1 (http://tree.bio.ed.ac.uk/software/figtree/). Net mean pairwise distances between

each mitochondrial group (uncorrected pairwise distance) were calculated using MEGA 6.06 (Tamura et al. 2013).

∂a∂i and ABBA-BABA Test

∂a∂i 1.6.3 (Gutenkunst et al. 2009) was used to infer the model of divergence between the nonadmixed *affinis* and *occisinensis* groups. We refiltered SNPs based on the aforementioned criteria for the nonadmixed *affinis* and *occisinensis* only, retaining a total of 15,624,147 SNPs. Ten divergence models with or without population size change were tested (supplementary fig. S2, Supplementary Material online): 1) strict isolation with no migration (SI), 2) strict isolation with no migration but with population size change (SI_pop), 3) isolation with symmetric migration (IsM), 4) isolation with symmetric migration and population size change (IsM_pop), 5) isolation with asymmetric migration (IaM), 6) isolation with asymmetric migration and population size change (IaM_pop), 7) secondary contact with symmetric migration (SCs), 8) secondary contact with symmetric migration and population size change (SCs_pop), 9) secondary contact with asymmetric migration (SCa), and 10) secondary contact with asymmetric migration and population size change (SCa_pop). The SI model indicates divergence between the two populations without gene flow; the IsM and IaM models indicate divergence with symmetric or asymmetric gene flow, respectively, while the SCs and SCa models indicate that the two populations first diverged in allopatry without gene flow, followed by a period of symmetric or asymmetric gene flow, respectively. All divergence models with population size change allowed for population size change from the split to the present for both *affinis* and *occisinensis*.

ABBA-BABA tests were conducted in ANGSD 0.902 (Korneliussen et al. 2014). We set nonadmixed *occisinensis* as P1, nonadmixed *affinis* as P2, *griseolus* as P3, and *P. sibilatrix* as the outgroup. D-statistic values with a Z-score >3 were retained. All individuals in each group were used for the ABBA-BABA test.

PSMC and LD Analyses

PSMC analysis (Li and Durbin 2011) was conducted with 100 bootstraps using three individuals (the intermediate individuals were excluded) with the highest sequencing depth from each taxon. The PSMC model estimates the time to the most recent common ancestor (TMRCA) of genome segments and infers N_e at a given time on the basis of the rates of the coalescent events and TMRCA distribution, thereby shedding light on historical demographic changes of a population (Li and Durbin 2011). A mutation rate of 0.33% per million years (Zhang et al. 2014) and generation time of 1.7 years (Bensch et al. 1999) were applied.

LD was estimated for each of the four groups (*griseolus*, nonadmixed *affinis*, and *occisinensis* and the intermediate group, see Results). We used the haplotype clustering based algorithm Beagle 4.1 (Browning and Browning 2007) to phase genotypes with the "gt" option. The phased genotypes were then used to estimate the correlation coefficient (r^2) between any two SNPs within 10-kb blocks as implemented in VCFtools 0.1.12b (Danecek et al. 2011) with the "−hap-r2"

and "–ld-window-bp 10000" options. Average r^2 within 100 bp was plotted against physical distance in R 3.3.3 (R Development Core Team 2008).

Sliding-Window Estimation of F_{ST}, D_{XY}, and RND

To obtain the chromosomal positions of SNPs, we mapped scaffolds from the reference genome of *P. sibilatrix* to the genome sequences of *Parus major* (Laine et al. 2016) using BLAST+ 2.2.26. To reduce possible mismatches, we used only scaffolds that had a single hit with an e-value $<10^{-40}$. We observed that ∼31% of scaffolds, containing ∼97.5% nucleotide sequences of the *P. sibilatrix* assembly, were mapped to *Parus major*. We used the same data set as that described for $\partial a \partial i$ analysis (refiltered SNPs for the nonadmixed *affinis* and *occinsensis* only, see above). We calculated F_{ST} (Weir and Cockerham 1984) and D_{XY} (Martin et al. 2015) between nonadmixed *affinis* and *occinsensis* in VCFtools 0.1.12b (Danecek et al. 2011) and the Python script egglib_sliding_windows.py (https://github.com/johnomics), respectively. Both F_{ST} and D_{XY} were estimated using 100-, 50-, 10-, and 2-kb nonoverlapping sliding windows, respectively. We defined outlier values of D_{XY} such that the absolute Z-score (standard score) values in a window were ≥ 3. The taxon *griseolus* could have constituted the donor lineage of D_{XY} outliers under the 2-kb window size between *affinis* and *occinsensis* as we detected historical gene flow between *affinis* and *griseolus* (see Results); therefore, we also calculated D_{XY} between *affinis* and *griseolus* using 2-kb nonoverlapping sliding windows. Additionally, to estimate measures of sequence divergence that are corrected for mutation rate variation, we calculated the RND (Feder el al. 2005) between nonadmixed *affinis* and *occinsensis* by dividing D_{XY} between them with the average D_{XY} between the focal taxa and the outgroup *P. trochiloides*.

Analysis of Hybrids

We used the R package HIest (Fitzpatrick 2012) to estimate hybrid index (S) and interspecific heterozygosity (H_I), allowing us to determine whether the seven intermediate individuals from the Lhasa–Nyingchi area (see Results) were early generation hybrids (F_1, F_2, first or second generation backcrosses). Only diagnostic markers ($F_{ST} = 1$, i.e., fixed SNPs distinguishing the parental groups *affinis* and *occinsensis*) extracted from the genome-wide SNP data set were used in this analysis. Because LD as measured by the correlation coefficient (r^2) decreased rapidly <0.2 within less than ∼500 bp (see Results), we only included SNPs separated by a distance >500 bp to reduce the bias introduced by linkage between markers. A total of 4,572 diagnostic SNPs with an average physical distance of ∼3,162 bp in each scaffold were used in this analysis.

Phenotypic Analysis

We measured morphometric traits, plumage colors, and songs to estimate phenotypic divergence between different groups within the *P. affinis* species complex.

To reduce observer bias, a single person (L.T.) measured six morphometric parameters: body mass, body length, tail length, wing length, tarsus length, and bill length (upper mandible to feathering) for a total of 120 specimens from the

National Zoological Museum, Institute of Zoology, Chinese Academy of Sciences, Beijing, including 35 *griseolus*, 63 nonadmixed *occinsensis*, 13 nonadmixed *affinis*, and 9 putatively intermediate individuals (supplementary table S6, Supplementary Material online). The nonadmixed *occinsensis* or *affinis* were defined as being from outside the Lhasa–Nyingchi area, while the putatively intermediate individuals represent individuals from the Lhasa–Nyingchi area (dashed lines in fig. 1a).

A single person (D.Z.) performed spectrophotometric measurements of crown, back, throat, and belly color of 109 specimens, including 26 *griseolus*, 46 nonadmixed *occinsensis*, 24 nonadmixed *affinis*, and 13 putatively intermediate individuals from the Lhasa–Nyingchi area (supplementary table S7, Supplementary Material online). We used an AvaSpec-ULS2048L-USB2 spectrophotometer (Avantes, Netherlands) with an average reading 3 and integration time 500 ms. The reflectance probe was held against the body at an angle of 90° at a distance of 2 mm and a measurement diameter of 6.5 mm. Three repetitive measurements from slightly different locations of each measuring position were taken. We retained wavelengths from 300 to 700 nm for subsequent analysis in the R package "pavo" (Maia et al. 2013). The "vismodel" function in "pavo" was used to calculate quantum catches Q_i in the avian retina, including ultraviolet wavelength sensitive Q_u, short wavelength sensitive Q_s, medium wavelength sensitive Q_m, and long wavelength sensitive Q_l (supplementary table S7, Supplementary Material online). The blue tit (*Cyanistes caeruleus*, Aves, Passeriformes, Paridae) was used as the visual model.

We conducted song analysis for a total of 178 individuals, including 39 *griseolus*, 97 nonadmixed *occinsensis*, 22 nonadmixed *affinis*, and 20 putatively intermediate individuals (supplementary table S8, Supplementary Material online). The song structure of members of the *P. affinis* complex generally contains two parts: part I is an introductory motif consisting of one or more simple notes, and part II contains multiple more complex notes (supplementary fig. S6, Supplementary Material online). A single person (L.T.) measured all song recordings in Avisoft-SASLab Pro 5.2.08 using the following 11 song parameters (supplementary table S8, Supplementary Material online): interval time between part I and part II (t1-2), duration of part II (t2), duration of a song (t), the maximum frequency of a song (Fmax), the minimum frequency of a song (Fmin), the maximum frequency of part I (F1-max), the minimum frequency of part I (F1-min), the maximum frequency of part II (F2-max), the minimum frequency of part II (F2-min), the number of notes in part I (N1), and the number of notes in part II (N2). Each parameter was averaged using all songs in a single recording from one individual.

We carried out LDA for morphometric, song, and plumage reflectance parameters, respectively, using the function "lda" in the R package "MASS" (Venables and Ripley 2002).

Supplementary Material

Supplementary data are available at *Molecular Biology and Evolution* online.

Acknowledgments

Author Contributions

The study program was conceived by F.L. and C.J., and experiments were designed by D.Z., F.L., C.J., and Y.Q. Sample collection was carried out by L.T. and J.C. The data were analyzed by D.Z., with assistance by L.T., Y.C., Y.H., F.E.R., G.S., and Y.X. The article was written by D.Z., F.E.R., P.A., and F.L.

References

Alcaide M, Scordato ES, Price TD, Irwin DE. 2014. Genomic divergence in a ring species complex. *Nature* 511(7507):83–85.

Alström P, Rheindt FE, Zhang R, Zhao M, Wang J, Zhu X, Gwee CY, Hao Y, Ohlson J, Jia C, et al. 2018. Complete species-level phylogeny of the leaf warbler (Aves: Phylloscopidae) radiation. *Mol Phylogenet Evol.* 126:141–152.

Avise JC. 2000. Phylogeography: the history and formation of species. Cambridge (MA) and London: Harvard University Press.

Bensch S, Andersson T, Åkesson S. 1999. Morphological and molecular variation across a migratory divide in willow warblers, *Phylloscopus trochilus. Evolution* 53(6):1925–1935.

Bhatia G, Patterson N, Sankararaman S, Price AL. 2013. Estimating and interpreting F_{ST}: the impact of rare variants. *Genome Res.* 23(9):1514–1521.

Bouckaert R, Heled J, Kuhnert D, Vaughan T, Wu CH, Xie D, Suchard MA, Rambaut A, Drummond AJ. 2014. BEAST 2: a software platform for Bayesian evolutionary analysis. *PLoS Comput Biol.* 10(4):e1003537.

Browning SR, Browning BL. 2007. Rapid and accurate haplotype phasing and missing-data inference for whole-genome association studies by use of localized haplotype clustering. *Am J Hum Genet.* 81(5):1084–1097.

Chevreux B, Wetter T, Suhai S. 1999. Genome sequence assembly using trace signals and additional sequence information. *Comput Sci Biol.* 99:45–56.

Clarke AL, Sæther B-E, Røskaft E, Saether B-E, Roskaft E. 1997. Sex biases in avian dispersal: a reappraisal. *Oikos* 79(3):429–438.

Clements JF, Schulenberg TS, Iliff MJ, Roberson D, Fredericks TA, Sullivan BL, Wood CL. 2018. The eBird/Clements checklist of birds of the world: v2018. Available from: http://www.birds.cornell.edu/clementschecklist/download/.

Currat M, Excoffier L. 2011. Strong reproductive isolation between humans and Neanderthals inferred from observed patterns of introgression. *Proc Natl Acad Sci U S A.* 108(37):15129–15134.

Currat M, Ruedi M, Petit RJ, Excoffier L. 2008. The hidden side of invasions: massive introgression by local genes. *Evolution* 62(8):1908–1920.

Dai C, Wang W, Lei F. 2013. Multilocus phylogeography (mitochondrial, autosomal and Z-chromosomal loci) and genetic consequence of long-distance male dispersal in Black-throated tits (*Aegithalos concinnus*). *Heredity* 110(5):457–465.

Danecek P, Auton A, Abecasis G, Albers CA, Banks E, DePristo MA, Handsaker RE, Lunter G, Marth GT, Sherry ST, et al. 2011. The variant call format and VCFtools. *Bioinformatics* 27(15):2156–2158.

del Hoyo J, Collar NJ. 2016. HBW and BirdLife International illustrated checklist of the birds of the world. Barcelona: Lynx Editions.

Durand EY, Patterson N, Reich D, Slatkin M. 2011. Testing for ancient admixture between closely related populations. *Mol Biol Evol.* 28(8):2239–2252.

Feder JL, Xie X, Rull J, Velez S, Forbes A, Leung B, Dambroski H, Filchak KE, Aluja M. 2005. Mayr, Dobzhansky, and Bush and the complexities of sympatric speciation in *Rhagoletis. Proc Natl Acad Sci U S A.* 102(Suppl 1): 6573–6580.

Fitzpatrick BM. 2012. Estimating ancestry and heterozygosity of hybrids using molecular markers. *BMC Evol Biol.* 12(1):131.

Fossøy F, Sorenson MD, Liang W, Ekrem T, Moksnes A, Moller AP, Rutila J, Roskaft E, Takasu F, Yang C, et al. 2016. Ancient origin and maternal inheritance of blue cuckoo eggs. *Nat Commun.* 7:10272.

Gill F, Donsker D. 2019. IOC World Bird List (v8.2). doi: 10.14344/IOC.ML.8.2.

Giska I, Sechi P, Babik W. 2015. Deeply divergent sympatric mitochondrial lineages of the earthworm *Lumbricus rubellus* are not reproductively isolated. *BMC Evol Biol.* 15(1):217.

Green RE, Krause J, Briggs AW, Maricic T, Stenzel U, Kircher M, Patterson N, Li H, Zhai W, Fritz MH, et al. 2010. A draft sequence of the Neandertal genome. *Science* 328(5979):710–722.

Gutenkunst RN, Hernandez RD, Williamson SH, Bustamante CD. 2009. Inferring the joint demographic history of multiple populations from multidimensional SNP frequency data. *PLoS Genet.* 5(10):e1000695.

Hahn C, Bachmann L, Chevreux B. 2013. Reconstructing mitochondrial genomes directly from genomic next-generation sequencing reads–a baiting and iterative mapping approach. *Nucleic Acids Res.* 41(13):e129.

Hajdinjak M, Fu Q, Hubner A, Petr M, Mafessoni F, Grote S, Skoglund P, Narasimham V, Rougier H, Crevecoeur I, et al. 2018. Reconstructing the genetic history of late Neanderthals. *Nature* 555(7698):652–656.

Heled J, Drummond AJ. 2010. Bayesian inference of species trees from multilocus data. *Mol Biol Evol.* 27(3):570–580.

Hogner S, Laskemoen T, Lifjeld JT, Porkert J, Kleven O, Albayrak T, Kabasakal B, Johnsen A. 2012. Deep sympatric mitochondrial divergence without reproductive isolation in the common redstart *Phoenicurus phoenicurus. Ecol Evol.* 2(12):2974–2988.

Huang DI, Hefer CA, Kolosova N, Douglas CJ, Cronk QC. 2014. Whole plastome sequencing reveals deep plastid divergence and cytonuclear discordance between closely related balsam poplars, *Populus balsamifera* and *P. trichocarpa* (Salicaceae). *New Phytol.* 204(3):693–703.

Huerta-Sánchez E, Jin X, Asan, Bianba Z, Peter BM, Vinckenbosch N, Liang Y, Yi X, He M, Somel M, et al. 2014. Altitude adaptation in Tibetans caused by introgression of Denisovan-like DNA. *Nature* 512(7513):194–197.

Irwin DE. 2002. Phylogeographic breaks without geographic barriers to gene flow. *Evolution* 56(12):2383–2394.

Irwin DE. 2012. Local adaptation along smooth ecological gradients causes phylogeographic breaks and phenotypic clustering. *Am Nat.* 180(1):35–49.

Johansson US, Alstrom P, Olsson U, Ericson PG, Sundberg P, Price TD. 2007. Build-up of the Himalayan avifauna through immigration: a biogeographical analysis of the *Phylloscopus* and *Seicercus* warblers. *Evolution* 61(2):324–333.

Korneliussen TS, Albrechtsen A, Nielsen R. 2014. ANGSD: Analysis of Next Generation Sequencing Data. *BMC Bioinformatics* 15(1):356.

Krosby M, Rohwer S. 2009. A 2000 km genetic wake yields evidence for northern glacial refugia and hybrid zone movement in a pair of songbirds. *Proc Biol Sci.* 276(1657):615–621.

Kuhlwilm M, Han S, Sousa VC, Excoffier L, Marques-Bonet T. 2019. Ancient admixture from an extinct ape lineage into bonobos. *Nat Ecol Evol.* 3(6):957–965.

Kvie KS, Hogner S, Aarvik L, Lifjeld JT, Johnsen A. 2012. Deep sympatric mtDNA divergence in the autumnal moth (*Epirrita autumnata*). *Ecol Evol*. 3(1):126–144.

Laine VN, Gossmann TI, Schachtschneider KM, Garroway CJ, Madsen O, Verhoeven KJ, de Jager V, Megens HJ, Warren WC, Minx P, et al. 2016. Evolutionary signals of selection on cognition from the great tit genome and methylome. *Nat Commun*. 7:10474.

Li H, Durbin R. 2009. Fast and accurate short read alignment with Burrows-Wheeler transform. *Bioinformatics* 25(14):1754–1760.

Li H, Durbin R. 2011. Inference of human population history from individual whole-genome sequences. *Nature* 475(7357):493–496.

Li H, Handsaker B, Wysoker A, Fennell T, Ruan J, Homer N, Marth G, Abecasis G, Durbin R, Genome Project Data Processing S. 2009. The Sequence Alignment/Map format and SAMtools. *Bioinformatics* 25(16):2078–2079.

Luo R, Liu B, Xie Y, Li Z, Huang W, Yuan J, He G, Chen Y, Pan Q, Liu Y, et al. 2012. SOAPdenovo2: an empirically improved memory-efficient short-read de novo assembler. *GigaScience* 1(1):18.

MacGuigan DJ, Near TJ. 2019. Phylogenomic signatures of ancient introgression in a rogue lineage of darters (Teleostei: Percidae). *Syst Biol*. 68(2):329–346.

Maia R, Eliason CM, Bitton P-P, Doucet SM, Shawkey MD, Tatem A. 2013. pavo: an R package for the analysis, visualization and organization of spectral data. *Methods Ecol Evol*. 4(10):906–913.

Martens J, Sun Y, Päckert M. 2008. Intraspecific differentiation of Sino-Himalayan bush-dwelling *Phylloscopus* leaf warblers, with description of two new taxa (*P. fuscatus*, *P. fuligiventer*, *P. affinis*, *P. armandii*, *P. subaffinis*). *Vertebr Zool*. 58(2):233–265.

Martin SH, Davey JW, Jiggins CD. 2015. Evaluating the use of ABBA-BABA statistics to locate introgressed loci. *Mol Biol Evol*. 32(1):244–257.

Olsson U, Alström P, Ericson PG, Sundberg P. 2005. Non-monophyletic taxa and cryptic species–evidence from a molecular phylogeny of leaf-warblers (*Phylloscopus*, Aves). *Mol Phylogenet Evol*. 36(2):261–276.

Päckert M, Martens J, Sun Y-H, Severinghaus LL, Nazarenko AA, Ting J, Töpfer T, Tietze DT. 2012. Horizontal and elevational phylogeographic patterns of Himalayan and Southeast Asian forest passerines (Aves: Passeriformes). *J Biogeogr*. 39(3):556–573.

Pavlova A, Amos JN, Joseph L, Loynes K, Austin JJ, Keogh JS, Stone GN, Nicholls JA, Sunnucks P. 2013. Perched at the mito-nuclear crossroads: divergent mitochondrial lineages correlate with environment in the face of ongoing nuclear gene flow in an Australian bird. *Evolution* 67(12):3412–3428.

Payseur BA, Rieseberg LH. 2016. A genomic perspective on hybridization and speciation. *Mol Ecol*. 25(11):2337–2360.

R Development Core Team. 2008. R: a language and environment for statistical computing. Vienna (Austria): R Foundation for Statistical Computing.

Reich DE, Cargill M, Bolk S, Ireland J, Sabeti PC, Richter DJ, Lavery T, Kouyoumjian R, Farhadian SF, Ward R, et al. 2001. Linkage disequilibrium in the human genome. *Nature* 411(6834):199–204.

Rheindt FE, Edwards SV. 2011. Genetic introgression: an integral but neglected component of speciation in birds. *Auk* 128(4):620–632.

Rohwer S, Bermingham E, Wood C. 2001. Plumage and mitochondrial DNA haplotype variation across a moving hybrid zone. *Evolution* 55(2):405–422.

Seixas FA, Boursot P, Melo-Ferreira J. 2018. The genomic impact of historical hybridization with massive mitochondrial DNA introgression. *Genome Biol*. 19(1):91.

She R, Chu JS, Wang K, Pei J, Chen N. 2008. GenBlastA: enabling BLAST to identify homologous gene sequences. *Genome Res*. 19(1):143–149.

Slater GS, Birney E. 2005. Automated generation of heuristics for biological sequence comparison. *BMC Bioinformatics* 6:31.

Spottiswoode CN, Stryjewski KF, Quader S, Colebrook-Robjent JFR, Sorenson MD. 2011. Ancient host specificity within a single species of brood parasitic bird. *Proc Natl Acad Sci U S A*. 108(43):17738–17742.

Tamura K, Stecher G, Peterson D, Filipski A, Kumar S. 2013. MEGA6: molecular evolutionary genetics analysis version 6.0. *Mol Biol Evol*. 30(12):2725–2729.

Tang H, Peng J, Wang P, Risch NJ. 2005. Estimation of individual admixture: analytical and study design considerations. *Genet Epidemiol*. 28(4):289–301.

Toews DP, Brelsford A. 2012. The biogeography of mitochondrial and nuclear discordance in animals. *Mol Ecol*. 21(16):3907–3930.

Toews DP, Taylor SA, Vallender R, Brelsford A, Butcher BG, Messer PW, Lovette IJ. 2016. Plumage genes and little else distinguish the genomes of hybridizing warblers. *Curr Biol*. 26(17):2313–2318.

Venables WN, Ripley BD. 2002. Modern applied statistics with S. New York: Springer.

Vilella AJ, Severin J, Ureta-Vidal A, Heng L, Durbin R, Birney E. 2008. EnsemblCompara GeneTrees: complete, duplication-aware phylogenetic trees in vertebrates. *Genome Res*. 19(2):327–335.

Webb WC, Marzluff JM, Omland KE. 2011. Random interbreeding between cryptic lineages of the Common Raven: evidence for speciation in reverse. *Mol Ecol*. 20(11):2390–2402.

Weir BS, Cockerham CC. 1984. Estimating F-statistics for the analysis of population-structure. *Evolution* 38(6):1358–1370.

Weir JT, Schluter D. 2008. Calibrating the avian molecular clock. *Mol Ecol*. 17(10):2321–2328.

Yang J, Lee SH, Goddard ME, Visscher PM. 2011. GCTA: a tool for genome-wide complex trait analysis. *Am J Hum Genet*. 88(1):76–82.

Zhang G, Li C, Li Q, Li B, Larkin DM, Lee C, Storz JF, Antunes A, Greenwold MJ, Meredith RW, et al. 2014. Comparative genomics reveals insights into avian genome evolution and adaptation. *Science* 346(6215):1311–1320.

Zhang W, Dasmahapatra KK, Mallet J, Moreira GR, Kronforst MR. 2016. Genome-wide introgression among distantly related *Heliconius* butterfly species. *Genome Biol*. 17:25.

Zink RM, Barrowclough GF. 2008. Mitochondrial DNA under siege in avian phylogeography. *Mol Ecol*. 17(9):2107–2121.